



Quantifying the periodicity of Heinrich and Dansgaard–Oeschger events during Marine Oxygen Isotope Stage 3

Authors: John A. Long and Paul Stoy

NOTICE: this is the author's version of a work that was accepted for publication in *Quaternary Research*. Changes resulting from the publishing process, such as peer review, editing, corrections, structural formatting, and other quality control mechanisms may not be reflected in this document. Changes may have been made to this work since it was submitted for publication. A definitive version was subsequently published in [Quaternary Research](#), volume 79, issue 3, May 2013, DOI#[10.1016/j.yqres.2013.02.003](#)

Long, John A., and Paul Stoy. "Quantifying the periodicity of Heinrich and Dansgaard–Oeschger events during Marine Oxygen Isotope Stage 3." *Quaternary Research* 79, no. 3 (2013): 413-423.

Made available through Montana State University's [ScholarWorks](#)
[scholarworks.montana.edu](#)

Quantifying the periodicity of Heinrich and Dansgaard–Oeschger events during Marine Oxygen Isotope Stage 3

John A. Long*, Paul C. Stoy

Department of Land Resources and Environmental Sciences, Montana State University, Bozeman, MT 59717, USA

ABSTRACT

Data from multiple ice and sediment cores in the North Atlantic show that Marine Oxygen Isotope Stage 3 (MIS 3) was characterized by recurring millennial-scale variations in climate, but the periodic behavior of the well-known millennial-scale variations, Heinrich events and Dansgaard–Oeschger events, is uncertain. We use oxygen isotope values from the Greenland Ice Sheet Project 2 (GISP2) and North Greenland Ice Core Project (NGRIP) ice cores and estimated sea-surface temperature derived from a Bermuda Rise marine sediment core as climate proxies to assess the periodic behavior of Heinrich events and Dansgaard–Oeschger events using Lomb–Scargle spectral decomposition and continuous time autoregressive models. We find that continuous time autoregressive models produce less variable estimates of periodicity for Heinrich events than Lomb–Scargle methods. Heinrich events during MIS 3 are periodic with an estimated periodicity of 6.29–6.49 ka in the GISP 2 ice core, 6.71–6.76 ka in the marine sediment core, and 7.89–8.23 ka in the NGRIP core. There is insufficient evidence from these data to conclude that Dansgaard–Oeschger events exhibit a single periodicity during MIS 3. We also find that the periodic behavior of millennial-scale variations depends on the observational time frame.

Introduction

The last glacial period in the Northern Hemisphere was characterized by repeated millennial-scale variations in climate (Olsen and Hammer, 2005) that are well-documented in glacial ice, marine, and terrestrial cores. Familiar millennial-scale climatic variations include Heinrich and Dansgaard–Oeschger (D–O) events. These are largely associated with Marine Oxygen Isotope Stage (MIS) 3, the period ~30–60 ka (*kilo annum*, 1 ka = 1000 yr) during the late Pleistocene. Forcing mechanisms are poorly understood, in part, because there is no consensus yet concerning their temporal characteristics (e.g., Thomas et al., 2011). The periodicity of Heinrich and, in particular, D–O events has been the subject of much debate (e.g., Grootes and Stuiver, 1997; Schulz, 2002; Ditlevsen et al., 2005). A more complete quantification of the periodicity of millennial-scale events is fundamental to a comprehensive understanding of past climate, which is critical to understanding current climate.

Heinrich events are quasi-periodic climate variations characterized by an extended period of cooling followed by a rapid shift to a warmer climate (Goldstein and Hemming, 2003). They have a recurrence interval between 6 and 7 ka, which is widely supported by ice-rafted debris (IRD) in marine sediment cores from the North Atlantic (e.g., Bond et al., 1999). The 6–7 ka recurrence interval is also

evident in marine sediment cores from non-North Atlantic sites (e.g., Gorbarenko et al., 2012), terrestrial sediment cores (e.g., Olsen and Hammer, 2005) and Greenland ice cores (e.g., Dergachev and van Geel, 2004). As the ice cores do not contain IRD, the 6–7 ka recurrence intervals are not, strictly speaking, Heinrich events, but are interpreted as such here. In this paper, we use the term “Heinrich event” to refer to variations directly evidenced with IRD in sediment cores as well as corresponding variation in ice cores.

There are competing theories regarding the cause of Heinrich events. Heinrich's original paper (1988) estimated the periodicity of the events at approximately 11 ka, which he attributed to one-half of the period of Earth's precession. Subsequent work has refined the timing and astronomical cycles are no longer thought to be primary forcing factors. One explanation is the binge–purge model (e.g., Hemming, 2004), which posits that an accumulation of ice (binge) on the Laurentide Ice Sheet during prolonged cooling periods eventually reached a critical mass, lubricating the land–ice boundary; the ice slid toward the sea, calving vast quantities of icebergs (purge). As the drifting icebergs melted, they deposited debris and injected a large amount of freshwater into the Atlantic that disrupted thermohaline circulation (Hemming, 2004).

D–O events, like Heinrich events, are climate oscillations with a more rapid recurrence interval of approximately 1–2 ka. They are characterized by an abrupt 6–10°C increase in air temperature over a short interval, often less than 50 yr (Dansgaard et al., 1993). D–O event identification is typically through temperature proxies, though lithic evidence exists in some marine sediment cores (e.g., Bond and

Lotti, 1995). They are thought to represent shifts between two different modes of the ocean–atmosphere system (Braun et al., 2010), but the precise mechanism is unclear. They are likely related to Heinrich events as both are associated with weakened circulation of North Atlantic Deep Water, and they are temporally related; each Heinrich event is followed by a series of progressively cooler D–O events until the start of the next Heinrich event (Rahmstorf, 2002; Dima and Lohmann, 2009).

Numerous studies have identified variation in climate proxies with a well-defined period of ~1.5 ka, the so-called millennial band, (e.g., Grootes and Stuiver, 1997; Rahmstorf, 2003) that has been associated with D–O events. For example, spectral analysis of oxygen isotope data from the Greenland Ice Sheet Project 2 (GISP2) core yielded a sharp peak with a period of 1.47 ka (Grootes and Stuiver, 1997). Others contend that: (1) there is insufficient support for periodicity in the GISP2 data (Ditlevsen et al., 2007; Thomas et al., 2011); (2) the variations are noise-induced and have limited predictability (Ditlevsen and Johnsen, 2010); or (3) the peak results from stochastic resonance in a bimodal climate system (Alley et al., 2001). Several researchers have shown that the periodicity of the millennial band depends on: (1) the source of the time series; for instance, the GISP2 core, the Greenland Ice Project (GRIP) core, or one of the many marine sediment cores (Hinnov et al., 2002; Ditlevsen et al., 2005); and (2) the time frame within a particular core (Hinnov et al., 2002; Schulz, 2002).

The purpose of this paper is to quantify the periodicity of Heinrich and D–O events during MIS 3 using oxygen isotope ($\delta^{18}\text{O}$) data and alkenone-derived estimates of sea-surface temperature (SST). SST and $\delta^{18}\text{O}$ are both common climate proxies with good consensus. We use the North Greenland Ice Core Project (NGRIP) and the GISP2 ice cores from Greenland, as well as a marine sediment core from the Bermuda Rise (BR) to ensure that observed periodicities reflect a hemispheric-scale rather than a regional response. We approach the problem of characterizing the periodic behavior of Heinrich events and D–O events from two statistical frameworks: (1) Lomb–Scargle spectral decomposition methods; and (2) continuous time autoregressive models. We note that our methods use linear frameworks, whereas others have used non-linear methods with similar ice-core records. Ditlevsen (1999), for example, used non-linear methods (Langevin equations) with the Greenland Ice Sheet Project (GRIP) core, whereas Kwasniok and Lohmann (2009) used unscented Kalman filtering with the NGRIP core. We examine whether Heinrich and D–O events are periodic and, if so, what is the associated period. Periodic behavior would imply a deterministic component (e.g., Thomas et al., 2011) and we discuss the implications of our results with respect to external climate forcing mechanisms and internal oscillations.

Methods

The GISP2 (72°36'N, 38°30'W) and the NGRIP (75°06'N, 42°19'W) are commonly studied ice cores from central Greenland (Fig. 1). The GISP2 core data are from the University of Washington's Quaternary Isotope Laboratory's GISP2 1 m data set and consist of an irregularly spaced time series of $\delta^{18}\text{O}$ measurements and their associated sample ages (Grootes et al., 1993; Meese et al., 1994; Stuiver et al., 1995; Grootes and Stuiver, 1997). This dataset spans the past 111 ka, but only the portion between 30 and 60 ka corresponding to MIS 3 was used. This portion is considered to be the full dataset and was designated G2(C). For analysis, subsets of the G2(C) data were created: (1) the front subset, G2(F), consisted of measurements from 30.03 to 49.94 ka; (2) the middle subset, G2(M), 34.05 to 54.05 ka; and (3) the tail subset, G2(T), 37.99–59.22 ka.

The NGRIP core data are from the Centre for Ice and Climate at the University of Copenhagen and consisted of a regularly spaced time series of $\delta^{18}\text{O}$ measurements and their associated sample ages (Andersen et al., 2006; Rasmussen et al., 2006; Svensson et al., 2006; Vinther et al., 2006; Svensson et al., 2008). This dataset spans the past 122 ka b2k, where b2k

is the notation adopted to mean 'years before A.D. 2000'; however, as with GISP2, only the portion between 30 and 60 ka was used. This portion is considered to be the full dataset and was designated NG(C). Subsets of the NG(C) data were also created: (1) the front subset, NG(F), consisted of measurements from 30.00 to 49.98 ka; (2) the middle subset, NG(M), 34.00 to 54.00 ka; and (3) the tail subset, NG(T), 38.00–60.00 ka.

The SST data, courtesy of the National Climatic Data Center, were from marine sediment core MD95–2036 from the Bermuda Rise (33°41'N, 57°35'W) in the Sargasso Sea (Fig. 1). The Bermuda Rise (BR) is a sediment drift deposit approximately 700 km northeast of the islands of Bermuda. Long-term temporal variations in SST near the BR are smaller than other places in the North Atlantic which has been taken as evidence that SSTs are indicative of a regional climate signal and not a localized climate response (Sachs and Lehman, 1999). The data consisted of an irregularly spaced time series of SSTs estimated from alkenone ratios (see Prahl and Wakeham, 1987), and associated sample ages derived by aligning features to the GISP2 ice core. Sample age was determined by maximizing the correlation between BR SST and variations in $\delta^{18}\text{O}$ using 146 tie-points, with an estimated uncertainty of 1.5–3.0 ka in absolute age (Sachs and Lehman, 1999). SST measurements are reported as within 0.17°C (1 σ) of their true values. The complete series from the Bermuda Rise, BR(C), spanned 31.75 to 61.22 ka. Subsets were created for the BR(C) data: (1) the front subset, BR(F), consisted of measurements from 31.75 to 49.92 ka; (2) the middle subset, BR(M), 34.00 to 54.12 ka; and (3) the tail subset, BR(T), 38.00–61.22 ka. It is important to note that the GISP2 and BR cores use the Meese–Sowers GISP2 time scale (Meese et al., 1997) whereas the NGRIP uses the Greenland Ice Core Chronology 2005 (GICC05) for dating.

Periodic patterns can be identified through spectral analysis, a set of methods that decompose a data series, here a time series, into its spectral components. Commonly used methods for spectral analysis include the Fast Fourier Transform (FFT) if the periodic patterns are stationary or wavelets if the patterns are non-stationary (i.e. the statistics of the time series change as a function of time); however, both methods assume that time series are evenly spaced, which is not typical with core data (Pardo-Iguzquiza and Rodríguez-Tovar, 2011). Interpolation schemes are often used to coerce irregularly sampled data into an evenly spaced series (e.g., Thomas et al., 2011), but we analyze the data at its native temporal resolution here.

The Lomb–Scargle (LS) algorithm is a spectral decomposition method that can support irregularly spaced time series (Ruf, 1999). Lomb (1976) showed that for unequally spaced data, a good approximation to the Fourier power spectrum was obtained by least squares fitting of sine waves to the data and then plotting the reduction in the sum of the residuals against frequency. This results in a least-squares power spectrum that quantifies the frequencies present in an unevenly spaced time series. Scargle (1982) extended this idea and suggested that for a sampled set $\{X(t_1), X(t_2), \dots, X(t_N)\}$ at frequency ω , the classical definition of spectral power

$$P_x(\omega) = \frac{1}{N} \left| \sum_{j=1}^N X(t_j) \exp^{-i\omega t_j} \right|^2 \quad (1)$$

$$= \frac{1}{N} \left[\left(\sum_{j=1}^N X_j \cos \omega t_j \right)^2 + \left(\sum_{j=1}^N X_j \sin \omega t_j \right)^2 \right]$$

could be replaced with

$$P_x(\omega) = \frac{1}{2} \left\{ \frac{\left[\sum_{j=1}^N X_j \cos \omega(t_j - \tau) \right]^2}{\sum_{j=1}^N \cos^2 \omega(t_j - \tau)} + \frac{\left[\sum_{j=1}^N X_j \sin \omega(t_j - \tau) \right]^2}{\sum_{j=1}^N \sin^2 \omega(t_j - \tau)} \right\} \quad (2)$$

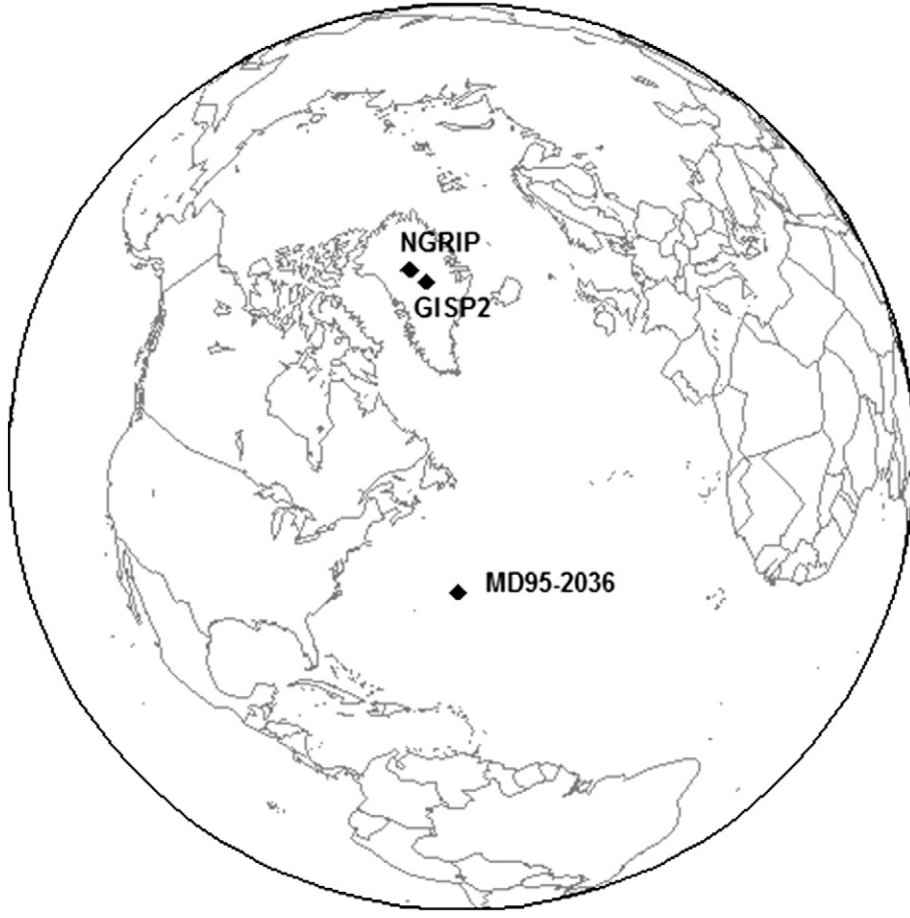


Figure 1. The GISP2 ice core (72°36'N, 38°30'W) and the NGRIP ice core (75°06'N, 42°19'W) are from central Greenland. The marine sediment core MD95-2036 (MD = *Marion Dufresne*, 95 = 1995, 2036 = core number 2036) was drilled in 1995 by the French research vessel *Marion Dufresne* and was taken from the Bermuda Rise (33°41'N, 57°35'W) in the Sargasso Sea (Bassiot and Labeyrie, 1995).

where τ , a time delay inserted to ensure invariance to time translation, is defined as

$$\tau = \left(\frac{1}{2\omega} \right) \tan^{-1} \left[\frac{\sum_{j=1}^N \sin(2\omega t_j)}{\sum_{j=1}^N \cos(2\omega t_j)} \right]. \quad (3)$$

This version is equivalent to Lomb's original and is invariant to time translation (Scargle, 1982). Plotting the spectral power against frequency gives the LS periodogram. The LS method can be used with any time series, including those that are evenly sampled, unevenly sampled, or have missing data. It minimizes bias and induced periodicities that might arise from interpolating missing values or forcing unevenly spaced data into an evenly spaced scheme, can efficiently identify peaks amid noisy data, does not show peaks at multiples of detected periodicities and can evaluate the likelihood that a given peak is the result of random fluctuations in power (Lomb, 1976; Scargle, 1982; Horne and Baliunas, 1986; Ruf, 1999). For these reasons it is a natural choice for quantifying periodicities in core data.

Initial exploration of the data indicated that a slight quadratic trend was present in each series. The presence of a trend causes non-stationarity since the mean changes as a function of time, but LS methods assume stationarity (Van Dongen et al., 1999). All data

were detrended and subsequent spectral analysis used LS methods on the residuals from the detrended models.

Variables related to climate are often correlated in time and we anticipated that temporal autocorrelation, if present, could produce false periodicities. The autoregressive moving-average, ARMA(p, q), time series for observations $\{x(t_1), x(t_2), \dots, x(t_N)\}$ with mean μ are given as:

$$x_t = \mu + \sum_{j=0}^p \alpha_j (x_{t-j} - \mu) + \sum_{i=0}^q \beta_i \varepsilon_{t-i} + \varepsilon_t \quad (4)$$

where α_j is the coefficient for an AR process of order p , β_i is the coefficient for an MA process of order q , and ε_t is noise error term (e.g., Koen, 2005). The AR(p) portion dominates in processes that operate on long time scales (Koen, 2005) such as the cores interpreted in this analysis; thus, Eq. (4) simplifies to:

$$x_t = \mu + \sum_{j=0}^p \alpha_j (x_{t-j} - \mu) + \varepsilon_t. \quad (5)$$

The AR model is time indexed with the implicit assumption that the time step is constant. This is not the case with unevenly sampled series.

Continuous time autoregressive (CAR) models are analogous to AR models. The salient difference is that AR(p) models are expressed as difference equations, while CAR(p) models are in terms of a linear

stochastic differential equation (SDE). A CAR model of order p , CAR(p), is defined in terms of the SDE

$$\alpha(D)Y(t) = \beta D\varepsilon(t) \quad (6)$$

where $Y(t)$ is a discrete time process; D is the differential operator where differentiation is with respect to t ; $\alpha(D) = D^p + \alpha_1 D^{p-1} + \dots + \alpha_p$; and $\varepsilon(t)$ is white noise. Thus, a CAR(3) process, for example, is defined as $(D^3 + \alpha_1 D^2 + \alpha_2 D + \alpha_3)Y(t) = \beta D\varepsilon(t)$. The parameters for the CAR model are the coefficients $\{\alpha_1, \alpha_2, \dots, \alpha_p\}$ of a stationary solution to Eq. (6). Belcher et al. (1994) and Koen (2005) provide further mathematical details.

Reparameterization of Eq. (6) based on the Cayley–Hamilton transformation, widely used to transform between continuous and discrete time, gives a new parameter space identical to stationary discrete time autoregressive models (Belcher et al., 1994). Parameters for the model, transformed in its new parameter space, are estimated with log-likelihood methods (see Belcher et al., 1994; Koen, 2005 for details). The importance for this paper is that the correlation r_k between observations $r_k = \frac{1}{c_0} \left(\frac{1}{N} \sum_{i=1}^{N-k} [x(t_i) - \mu][x(t_{i+k}) - \mu] \right)$ is in terms of k , the difference in time indices, rather than in time intervals (Koen, 2005). Thus, CAR(p) models are well-suited to address temporal autocorrelation in unevenly sampled time series such as core-derived data (Belcher et al., 1994). We fit CAR models of varying orders using the Continuous Time Autoregressive Models (cts) package in R (R Development Core Team, 2011). The best fitting CAR model was selected by Akaike Information Criterion (AIC). As in the LS approach, CAR models were fit to the residuals from detrended models.

Periods are the inverses of frequency at the point of maximum spectral power density SPD_{\max} . The half-power bandwidth (W_b) is the width of a spectral peak measured at the half spectral power point $SPD_{\max}(2)^{-1/2}$ (Liu et al., 2011); it is used here as a measure of variability and to derive upper and lower bounds for a given period.

Results

We begin by illustrating the agreement between the respective climate proxies (Fig. 2). All major climate variations observed in the GISP2 ice core are evident in the BR SST series. This is not surprising since the ages for the BR were derived by maximizing the correlation ($r = 0.83$) between BR SSTs and layer-counted variations in the GISP2 ice core (Sachs and Lehman, 1999) but not the NGRIP core. D–O events identified in Greenland ice cores using $\delta^{18}\text{O}$ values are closely matched by North Atlantic SST records (Bond et al., 1993) and, within dating uncertainties, by the BR core (Keigwin and Boyle, 1999). The major climate variations are also evident in the NGRIP core, but alignment differs due to differences in time scales.

The GICC05 is a relatively new composite stratigraphic time scale developed from three Greenland ice cores (Andersen et al., 2006; Rasmussen et al., 2006; Svensson et al., 2006; Vinther et al., 2006; Svensson et al., 2008). The GISP2 and GICC05 time scales agree within the GICC05's counting uncertainty (1σ) for the period 30–43 ka (Svensson et al., 2008). During the period 43–60 ka, the GISP2 time scale consistently gives ages younger than the GICC05 time scale; age estimates exceed GICC05 uncertainty bounds by as much as 1.5 ka at approximately 52 ka (Svensson et al., 2008).

Quantifying periodicity using the LS method

Spectral analysis of $\delta^{18}\text{O}$ measurements from the GISP2 core using LS methods indicates that periodicities corresponding to reported recurrence intervals for Heinrich and D–O events are present in the data (Fig. 3a). The likelihood that the labeled peaks are due to random fluctuations (chance) in spectral power is less than 5%; whereas chance occurrence of the unlabeled peaks exceeds 5%. The periodicity of Heinrich events is estimated at 6.05 ka ($W_b = 0.9$ ka); however, the periodicity of D–O events is less conclusive. Their periodicity is estimated to be 1.43 ka ($W_b = 0.04$ ka); however, this is the dominant

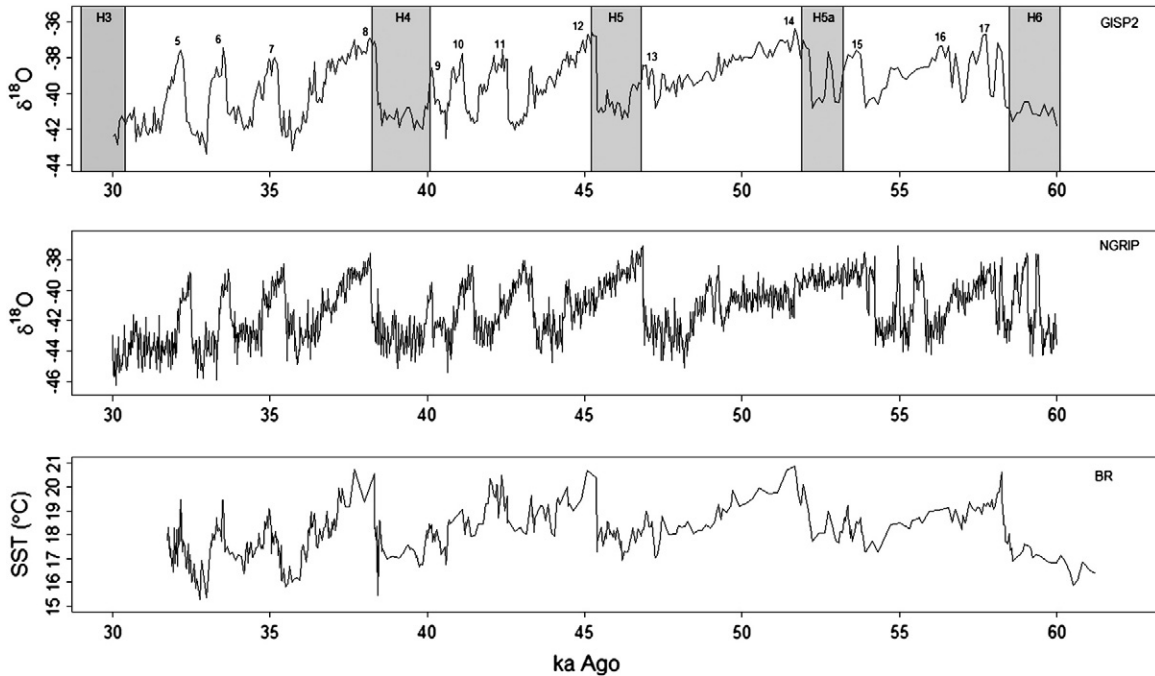


Figure 2. The chronology of millennial-scale climate variations (top) during Marine Oxygen Isotope Stage 3 (30–60 ka) superimposed over oxygen isotope ($\delta^{18}\text{O}$) values derived from the Greenland Ice Sheet Project 2 (GISP2) core. The use of $\delta^{18}\text{O}$ as a climate proxy is common and is scaled here such that less negative values are associated with warmer temperatures. This period includes 5 Heinrich events and 13 Dansgaard–Oeschger events. The Heinrich events: H3, H4, H5, H5a, and H6, are the broad shaded bands (dates are from Hemming, 2004) and are derived from sediment cores using ice raft debris, while the Dansgaard–Oeschger events are the peaks numbered D–O 5 through D–O 17 (dates are from Blunier and Brook, 2001). The $\delta^{18}\text{O}$ values for the NGRIP core (middle) are similarly scaled. The estimated sea-surface temperature from the Bermuda Rise core (bottom) is shown for the same time period.

period in a partially resolved doublet (the other is at 1.51 ka), suggesting that either the periodicity is closer to the reported value of 1.47 ka or there are multiple periodicities. Given the considerable disagreement on the precise periodicity of D–O events, the sizeable peaks at 1.65 ka cannot be characterized as unrelated. Furthermore, we are unable to claim that the peaks at 2.58, 3.16, and 3.95 ka are unrelated to D–O events in light of research supporting a possible non-linear dynamical process that leads to multimodal behavior (e.g., Braun et al., 2011).

Results from the LS analysis of the GISP2 subsets suggest that the characterization of periodicity of millennial-scale climate variability during MIS 3 is influenced by the data's time frame. Table 1 summarizes periodicity for all data using LS methods. Periodicities corresponding to the reported values for Heinrich events and D–O events exist in all data subsets from the GISP2 core; however, their specific values and relative strengths vary (Figs. 3b, c, and d). Periodicity estimates for Heinrich events range from 6.01 to 6.61 ka, while estimates for D–O event periodicity are from 1.40 to 1.46 ka. As with the full series, sizeable peaks of intermediate periodicity exist at ~2–4 ka.

Spectral analysis of SST measurements from the BR sediment core using LS methods also indicates that periodicities corresponding to reported recurrence intervals for Heinrich and D–O events are present in the data (Fig. 4a). Considering the complete series, BR(C), the periodicity for Heinrich events is estimated at 6.69 ka ($W_b = 0.77$ ka). The periodicity of D–O events is estimated at 1.44 ka ($W_b = 0.04$ ka), which is, as in the GISP2 core, one period in a partially resolved doublet; the other period is at 1.53 ka. This, again, suggests that the periodicity in these data might be closer to the reported value of 1.47 ka or that multiple periodicities exist. Support for D–O events in the BR core is weaker than that found in the GISP2 core when measured by spectral power. Multiple peaks exist at ~2–4 ka as found in the GISP2 core, though these differ in number and periodicity (Table 1).

Subsets of the BR data produce results similar to those from the GISP2 core in that the characterization of millennial-scale periodicity during MIS 3 is influenced by the data's time frame. The number of periodicities, values, and relative strengths varies according to which subset of the data is used (Table 1). The complete series, BR(C), is noisy and many of the periods are partially resolved doublets and triplets (Figs. 4b, c, and d). Periodicities corresponding to reported periodicities for Heinrich events and D–O events exist in all data subsets from the BR sediment core. Periodicity estimates for Heinrich events range from 6.53 to 7.01 ka, while estimates for D–O event periodicity are from 1.44 to 1.58 ka. Multiple peaks persist at ~2–4 ka.

Spectral analysis of $\delta^{18}\text{O}$ measurements from the NGRIP core with the LS method gives periodicities that correspond approximately to the reported recurrence intervals for Heinrich and D–O events (Fig. 5a). Considering the complete series, NG(C), Heinrich event periodicity is estimated at 8.54 ka ($W_b = 0.81$ ka). The peak at 8.54 ka suggests a longer recurrence interval for Heinrich events than typically found in the literature and is likely a result of differences in time scale. GICC05 derived ages are older than those derived from the GISP2 time scale for half of MIS 3; thus, it is not unreasonable to expect corresponding shifts in periodicity. D–O event periodicity in the full series is difficult to assess as there are at least four peaks between 1.27 ka and 1.57 ka. The dominant periodicity is 1.57 ka ($W_b = 0.03$ ka) and, considering the GICC05 time scale, corresponds most closely to the reported periodicities for D–O events. Support for a single periodicity associated with D–O events is weak in NGRIP core when measured by spectral power. Multiple peaks persist at ~2–4 ka as in the other cores, though these differ in number and periodicity (Table 1).

Subsets of the NGRIP data produce results similar to the GISP2 and BR cores in that the characterization of millennial-scale periodicity during MIS 3 depends on the data's time frame. The number of identified periodicities, values, and relative strengths differ according to subset. The

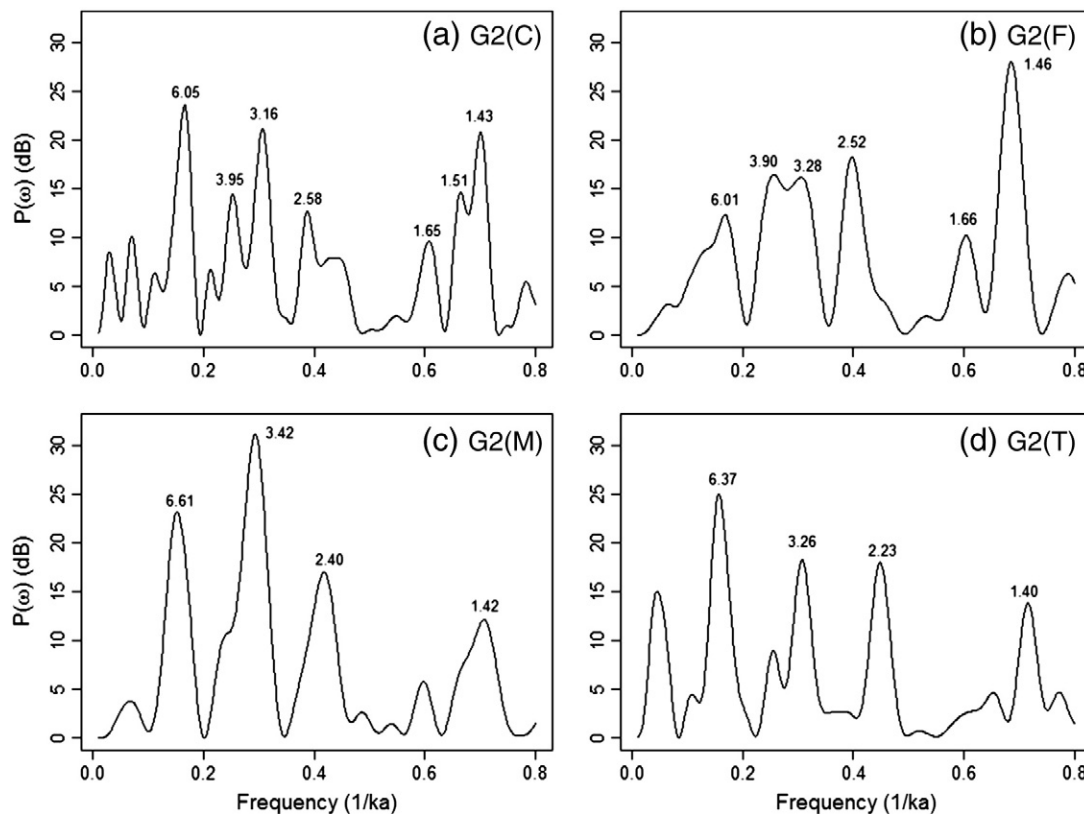


Figure 3. Lomb–Scargle periodograms from the GISP2 data: (a) the complete data series [G2(C) 30.03–59.99 ka]; (b) the front subset [G2(F) 30.03–49.94 ka]; (c) the middle subset [G2(M) 34.05–54.05 ka]; and (d) the tail subset [G2(T) 37.99–59.99 ka]. Labeled peak periodicities are measured in ka and the probability of their chance occurrence is less than 5%.

Table 1
Periodicity estimates from Lomb–Scargle spectral decomposition.

Data ^a	Periodicities (ka)												
G2(C)	6.05	3.95	3.16	2.58	1.65	1.51	1.43						
G2(F)	6.01	3.90	3.28	2.52	1.66	1.46							
G2(M)	6.61	3.42	2.40	1.42									
G2(T)	6.37	3.26	2.23	1.40									
BR(C)	6.69	4.89	4.01	3.46	2.61	1.89	1.77	1.65	1.53	1.44			
BR(F)	6.53	3.68	2.66	1.78	1.47								
BR(M)	6.58	4.55	3.60	2.51	1.82	1.50							
BR(T)	7.01	5.05	3.33	1.58									
NG(C)	8.54	5.96	4.95	4.02	2.89	2.64	2.26	1.97	1.80	1.57	1.41	1.34	1.27
NG(F)	8.90	4.26	2.82	1.87	1.53	1.38	1.29						
NG(M)	8.10	3.96	2.81	2.27	1.88	1.54							
NG(T)	8.50	5.29	3.94	2.94	2.55	2.11	1.76	1.59					

^a G2(C), the portion of the GISP2 ice core from Marine Oxygen Isotope Stage 3 (30.03–59.99 ka); G2(F), the front portion of the GISP2 core (30.03–49.94 ka); G2(M), the middle portion of the GISP2 core (34.05–54.05 ka); G2(T), the tail portion of the GISP2 core (37.99–59.99 ka); BR(C), the complete data set for the Bermuda Rise time series (31.75–61.22 ka); BR(F), the front portion of the Bermuda Rise data (31.75–49.92 ka); BR(M), the middle portion of the Bermuda Rise data (34.00–54.12 ka); BR(T), the tail portion of the Bermuda Rise data (38.00–61.22 ka); NG(C), the portion of the NGRIP ice core from Marine Isotope Stage 3 (30.00–60.00 ka); NG(F), the front portion of the NGRIP core (30.00–49.98 ka); NG(M), the middle portion of the NGRIP core (34.00–54.00 ka); NG(T), the tail portion of the NGRIP core (38.00–60.00 ka).

complete series, NG(C), is noisy and several of the periods are partially resolved doublets or have low spectral power (Figs. 5b, c, and d). Periodicities corresponding to reported values for Heinrich events and D–O events exist in all data subsets from the NGRIP ice core. Estimates for Heinrich events range from 8.10 to 8.90 ka, while estimates for D–O event periodicity are from 1.53 to 1.59 ka. Multiple peaks persist at ~2–4 ka and cannot be excluded as unrelated.

Quantifying periodicity using CAR models

The data from all cores are temporally autocorrelated. Spectral analysis of the GISP2 core after filtering with CAR models reduces

much of the noise in the respective series and eliminates many periodicities. Spectral analysis of the best fitting model, CAR(11), for the G2(C) series indicates that periodicities corresponding to reported recurrence intervals for Heinrich and D–O events persist in the data after filtering (Table 2). The periodicity corresponding to Heinrich events is estimated at 6.41 ka (Fig. 6a) and is less variable at the half-power points ($W_b = 0.20$ ka) than the corresponding LS estimate. D–O event periodicity is estimated at 1.69 ka ($W_b = 0.14$ ka). Filtering eliminated all but one of the peaks, 3.62 ka, in the 2–4 ka region.

The G2(F), G2(M), and G2(T) subsets of the GISP2 data use CAR(11), CAR(9), and CAR(9) models respectively. Heinrich event

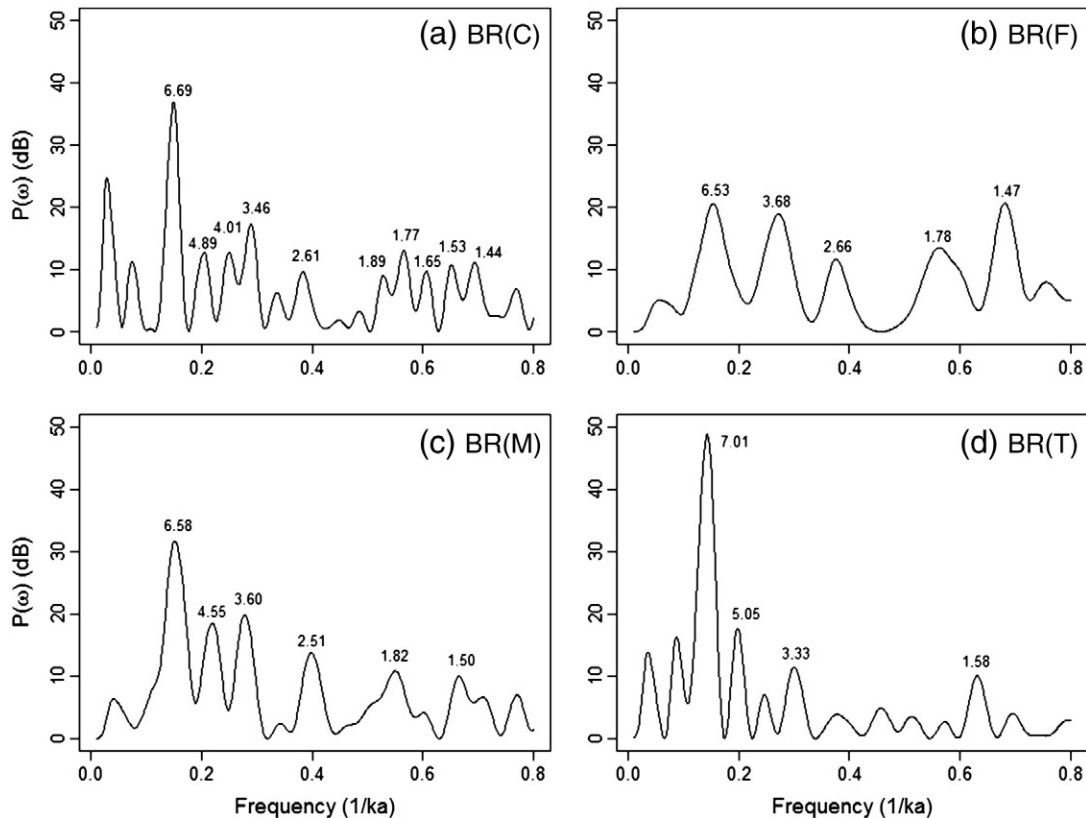


Figure 4. The same as Fig. 3 but for the Bermuda Rise sediment core: (a) the complete data series [BR(C) 31.75–61.22 ka]; (b) the front subset [BR(F) 31.75–49.92 ka]; (c) the middle subset [BR(M) 34.00–54.12 ka]; and (d) the tail subset [BR(T) 38.00–61.22 ka].

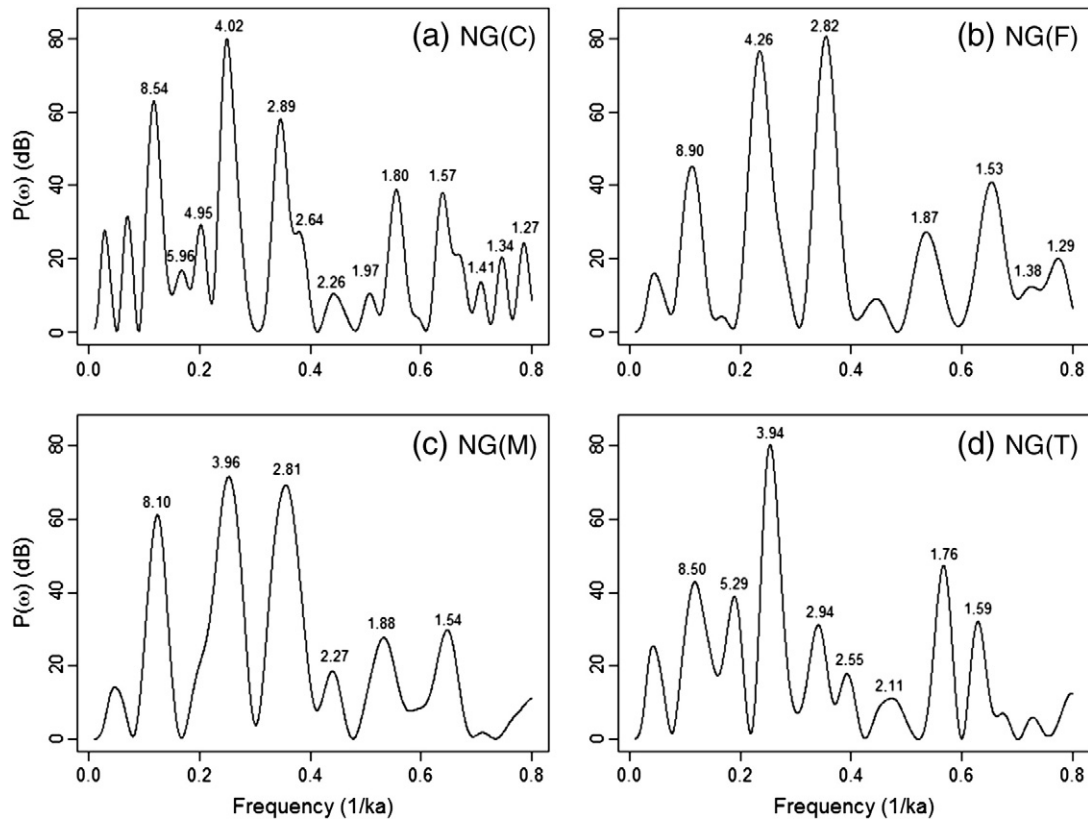


Figure 5. The same as Fig. 3 but for the NGRIP ice core: (a) the complete data series [NG(C) 30.00–60.00 ka]; (b) the front subset [NG(F) 30.00–49.98 ka]; (c) the middle subset [NG(M) 34.00–54.00 ka]; and (d) the tail subset [NG(T) 38.00–60.00 ka].

periodicity is evident in each of these subsets (Figs. 6b, c, and d) and estimates range from 5.88 to 6.45 ka. In all cases, the periods are more sharply defined (smaller W_b) than the corresponding LS estimates. Periodicity for D–O events continues to be dependent on the subset’s time frame. It is estimated at 1.63 ka in the G2(F) series, but it is a relatively wide ($W_b = 0.74$) peak in the periodogram. Wide peaks are indicative of diffuse spectral power and suggest multiple or ill-defined periodicities. D–O periodicity is not supported in the G2(M) and G2(T) series, further corroborating the claim that the periodicity of millennial-scale variations during MIS 3 is dependent on the data’s time frame. As with the complete series, a peak at ~ 3.5 ka persists in each GISP2 subset.

Spectral analysis of the BR sediment core after filtering with CAR models gives results similar to those from the corresponding GISP2

series (Table 2). Heinrich event periodicity in the BR(C) series is estimated at 6.71 ka from a CAR(14) model. This period is sharply defined ($W_b = 0.05$) in the periodogram (Fig. 7a). D–O event periodicity is estimated at 1.51 ka, but, as in the GISP2 core, it is a wide ($W_b = 0.62$) and poorly defined peak in the periodogram. A single intermediate peak persists at ~ 3.7 ka. The BR(F), BR(M), and BR(T) subsets use CAR(10), CAR(12), and CAR(10) models respectively and results are similar to those from the GISP2 core. Estimates of Heinrich event periodicity in the BR subsets range from 6.29 to 6.76 and have narrow peaks in the periodogram (Figs. 7b, c, and d). Periodicity for D–O events is estimated at 1.76 ka in the BR(F) and BR(M) series, but these are broad ($W_b = 0.65$ and 0.84 respectively) with poorly defined periods. D–O periodicity is not supported in the BR(T) series. Once again, a single intermediate period persists at ~ 2.5 – 3.7 ka, depending on the subset.

Spectral analysis of the NGRIP core using the best fitting model, CAR(13) for the NG(C) series, indicates that periodicities corresponding to reported recurrence intervals for Heinrich and D–O events remain evident in the data after filtering (Table 2). Heinrich event periodicity is estimated at 8.06 ka and is less variable ($W_b = 0.17$ ka) than the corresponding LS estimate. D–O event periodicity (Fig. 8a) is estimated at 1.59 ka ($W_b = 0.12$ ka) and remains poorly defined. Most of the peaks with intermediate periodicities were eliminated. The NG(F), NG(M), and NG(T) subsets use CAR(12), CAR(10), and CAR(12) models respectively. Heinrich event periodicity is evident in each subset (Figs. 8b, c, and d) and estimates range from 7.75 to 10.20 ka. The periods for all subsets are more sharply defined (smaller W_b) than the corresponding LS estimates. Periodicity for D–O events continues to be variable and dependent on the time frame. It is estimated at 1.53 ka in the NG(F) series, 2.16 ka in the NG(M) series, and 1.90 ka in the NG(T) series. As with the complete series, peaks at ~ 2 – 4 ka persist in each subset.

Table 2
Periodicity estimates from continuous autoregressive (CAR) models.

Data ^a	Periodicities (ka)			
G2(C)	6.41	3.62	1.69	
G2(F)	5.88	3.53	1.63	
G2(M)	6.37	3.48		
G2(T)	6.45	3.7		
BR(C)	6.71	3.66	1.51	
BR(F)	6.29	3.64	1.68	
BR(M)	6.67	3.69	1.76	
BR(T)	6.76	2.43		
NG(C)	8.06	4.46	3.14	1.59
NG(F)	10.20	4.37	3.16	1.53
NG(M)	7.75	4.00	2.16	
NG(T)	7.87	4.22	1.90	

^a Same as Table 1.

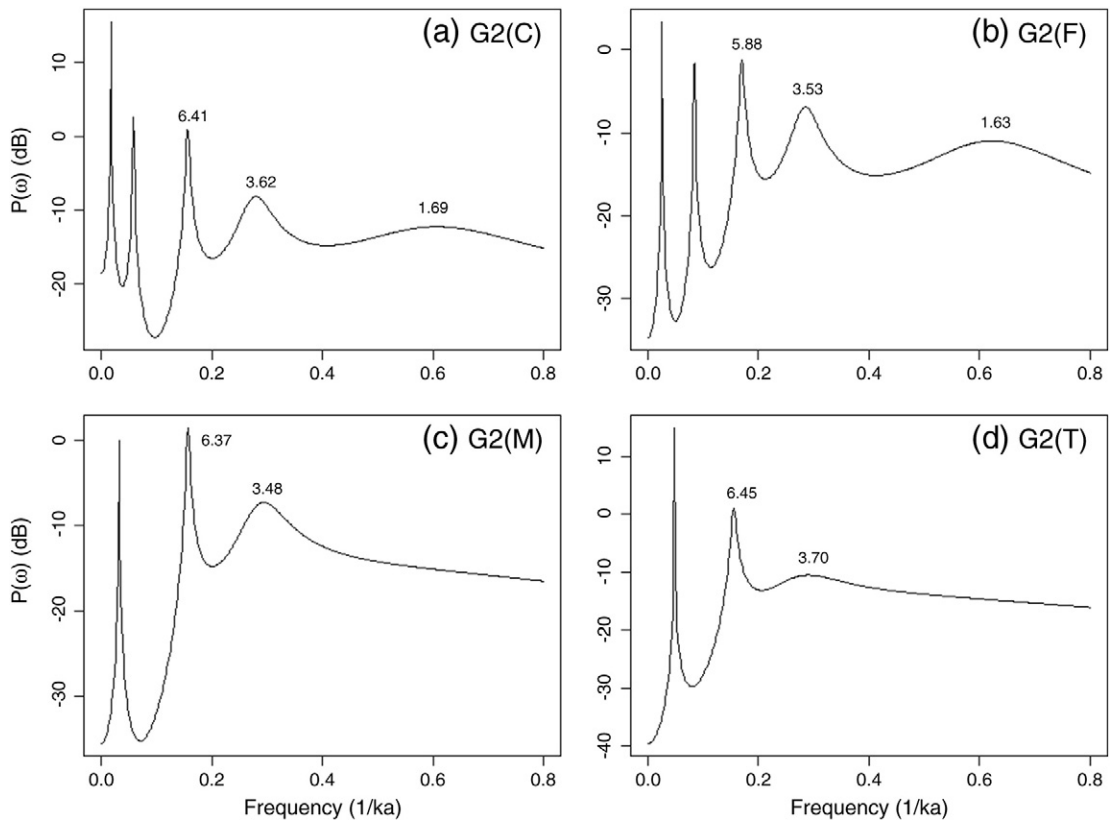


Figure 6. Periodograms of the continuous autoregressive (CAR) models from the GISP2 data: (a) the complete data series [G2(C) 30.03–59.99 ka]; (b) the front subset [G2(F) 30.03–49.94 ka]; (c) the middle subset [G2(M) 34.05–54.05 ka]; and (d) the tail subset [G2(T) 37.99–59.99 ka]. The labeled peaks are those that remain after accounting for temporal autocorrelation and are measured in ka.

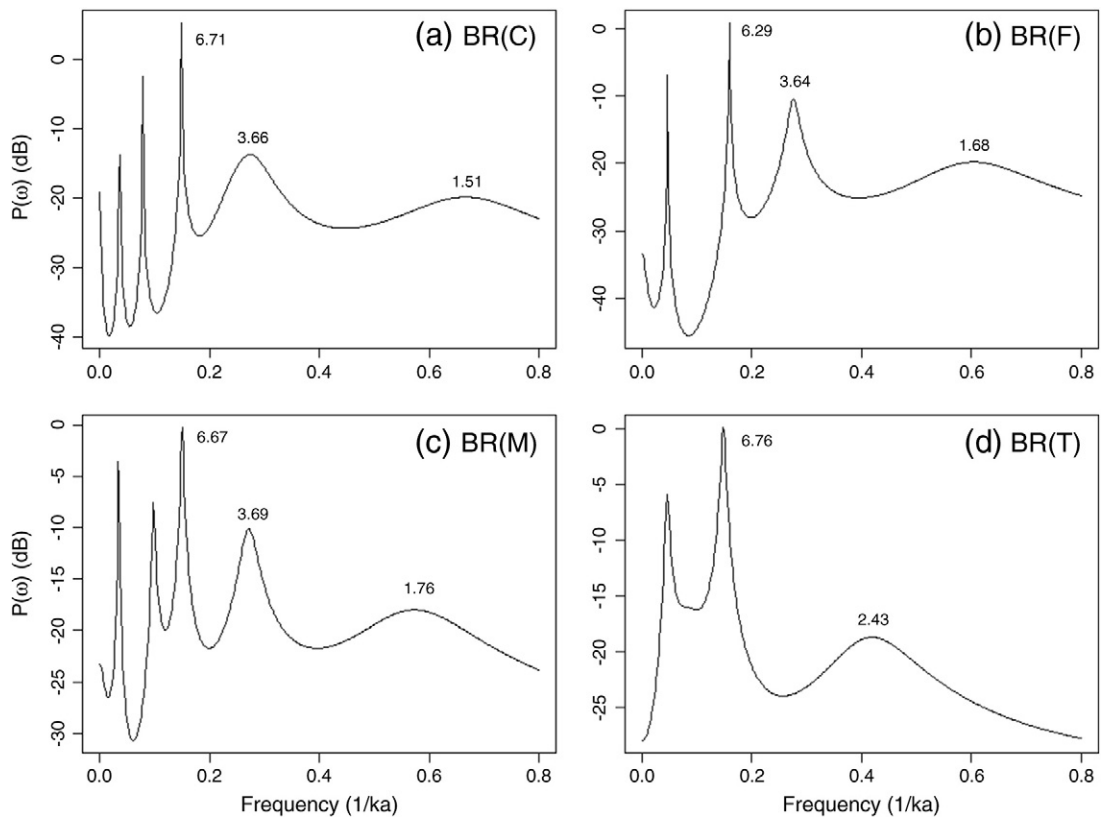


Figure 7. The same as Fig. 6 but for the Bermuda Rise data: (a) the complete data series (31.75–61.22 ka); (b) the front subset (31.75–49.92 ka); (c) the middle subset (34.00–54.12 ka); and (d) the tail subset (38.00–61.22 ka).

Discussion

The spectral analyses performed here support claims that Heinrich events during MIS 3 are periodic with a recurrence interval of 6–7 ka on the Meese-Sowers GISP2 time scale or approximately 8 ka on the GICC05 time scale. LS spectral decomposition methods and the spectral analysis of CAR models reveal peaks in the periodograms that correspond to reported estimates of Heinrich event periodicity (e.g., Clement and Peterson, 2008; Pias et al., 2010). These peaks are sharper when analyzing the data with CAR models than LS-derived estimates. Heinrich event periodicity is evident in the GISP2 ice core, the BR sediment core, and the NGRIP ice core, suggesting that this signal is robust with respect to climate proxy; it is present in $\delta^{18}\text{O}$ measurements and SST estimates. It is also robust with respect to time scale (Table 1).

We estimate that Heinrich events reoccurred during MIS 3 with a periodicity of 6.29–6.49 ka based on the GISP2 core. The corresponding estimate based on the BR core is 6.71–6.76 ka. Both intervals are estimated from the spectral analysis of their respective CAR models and are measured at the W_b ; differences in periodicity arise despite the fact that the BR time scale was derived from the GISP2 ice core. Heinrich event periodicity is estimated at 7.89–8.23 ka based on the NGRIP core. Disparities in the identification in Heinrich event periodicity should be addressed by interpreting multiple cores with the best possible temporal dating. Furthermore, evidence that Heinrich events are periodic does not depend on a particular subset of the dates in MIS 3; data from the complete series and all subsets suggest that Heinrich events are periodic. Subsets differ, however, in quantifying the period. The consistent behavior of the Heinrich event signal suggests a periodic external forcing mechanism operating on a similar temporal scale.

The evidence for D–O event periodicity during MIS 3 is less conclusive. LS methods consistently indicate a periodicity at ~ 1.5 ka regardless of which core is used and whether the full data series or a subset is used, but spectral analysis of the CAR models does not agree. For LS methods, the spectral peaks corresponding to the reported periodicity for D–O events are less definitive than those for Heinrich events and are often the dominant peak in a partially resolved doublet; for example, in the complete series for GISP2 core and the BR core. In both instances, averaging the periods of the doublet components gives estimates for D–O event periodicity that closely match reported results (e.g., Grootes and Stuiver, 1997). Furthermore, there are often nearby peaks with appreciable spectral power which cannot be easily dismissed. Whether they result from time-scale inaccuracies, represent additional periods as a consequence of internal oscillations, or are entirely unrelated is unknown.

Spectral analysis of the CAR models reveals two important findings regarding D–O events: (1) spectral peaks that correspond to the reported periodicity of D–O events are weak and broad; and (2) the periodic behavior of D–O events depends on the particular data subset. This is the case for all cores. A broad peak results when the spectral power is spread out over a range of frequencies; thus, the signal is weak and periodicity is not consistent. We estimate that D–O events reoccurred during MIS 3 with a periodicity of 1.25–1.39 ka based on the GISP2 core, 1.25–1.87 ka based on the BR core, and 1.47–1.71 ka based on the NGRIP core. All intervals are estimated from the spectral analysis of their respective CAR models and are measured at the W_b . These findings are in agreement with a 1.5–2.5 ka average period discussed by others (e.g., Olsen and Hammer, 2005).

D–O events are not present in all subsets when using CAR models; they are absent in the G2(M), G2(T) and BR(T) subsets. This leads us to conclude that, unlike Heinrich events, the periodic behavior of D–O events during MIS 3 depends on the data's time frame. The existence

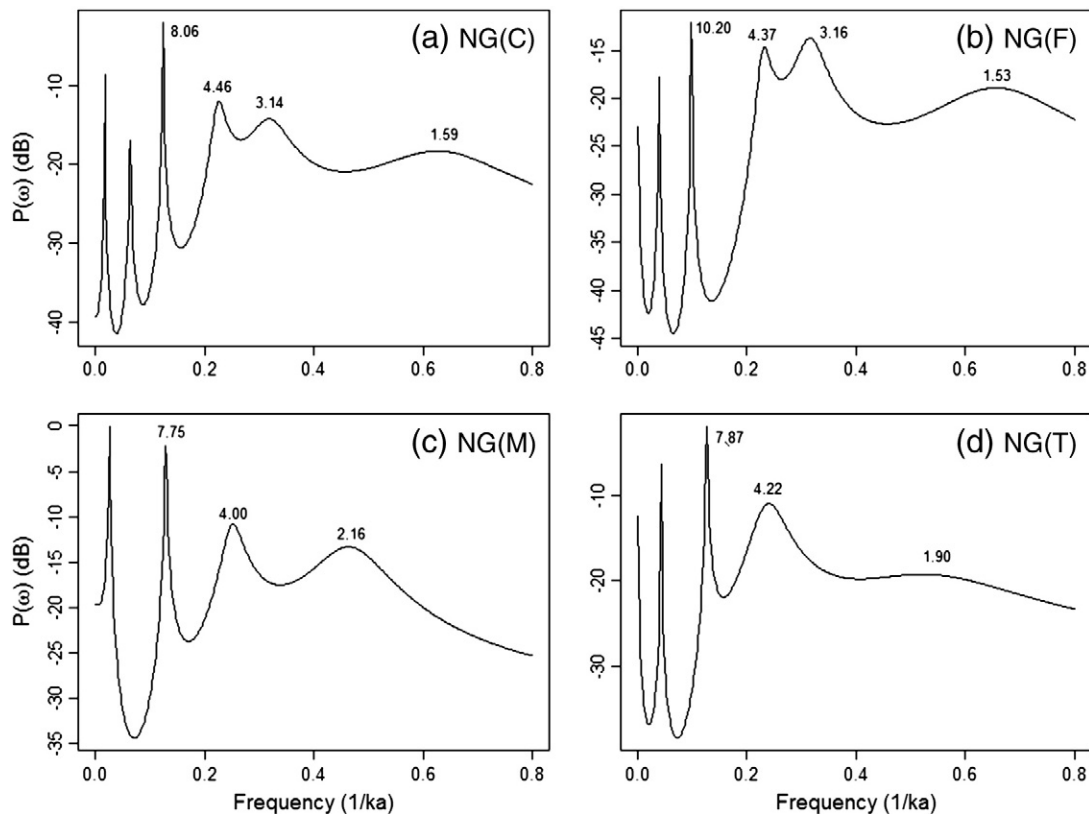


Figure 8. The same as Fig. 6 but for the NGRIP ice core: (a) the complete data series [NG(C) 30.00–60.00 ka]; (b) the front subset [NG(F) 30.00–49.98 ka]; (c) the middle subset [NG(M) 34.00–54.00 ka]; and (d) the tail subset [NG(T) 38.00–60.00 ka].

of a persistent period at ~2–4 ka, regardless of data series, from the CAR models is intriguing. We feel unjustified in suggesting that these peaks are unrelated to D–O events considering research supporting potential non-linear stochastic processes that lead to multimodal behavior of D–O events (e.g., Braun et al., 2011).

The periodic nature of D–O events has been much debated. A substantial body of work has suggested that D–O events are periodic (e.g., Grootes and Stuiver, 1997; Rahmstorf, 2002). Others have cited a lack of evidence to claim that the D–O signal was cyclical (e.g., Ditlevsen et al., 2005; Thomas et al., 2011). We conclude that there is insufficient evidence in either the GISP2 ice core, the Bermuda Rise sediment core, or the NGRIP ice core to claim that D–O events exhibit a single periodicity during MIS 3. We do not mean to imply that D–O events do not exist, only that the data indicate that they are likely not driven by forcing with a single periodicity.

Acknowledgments

We thank the Quaternary Isotope Laboratory at the University of Washington, the Centre for Ice and Climate at the University of Copenhagen, and the World Data Center for Paleoclimatology for making their respective data sets available online; as well as the Stowers Institute for Medical Research (Glynn et al., 2005) for the Lomb–Scargle R-code. We additionally thank Dr. Peter Ditlevsen, an anonymous reviewer, and Dr. Alan Gillespie for valuable comments on the manuscript, and Dr. Tracy Sterling and the Montana State University Department of Land Resources and Environmental Sciences for financial assistance. PCS acknowledges support from the National Science Foundation ('Scaling ecosystem function: Novel Approaches from MaxEnt and Multiresolution', DBI #1021095).

References

- Alley, R.B., Anandakrishnan, S., Jung, P., 2001. Stochastic resonance in the North Atlantic. *Paleoceanography* 16 (2), 190–198. <http://dx.doi.org/10.1029/2000PA000518>.
- Andersen, K.K., Svensson, A., Johnsen, S.J., Rasmussen, S.O., Bigler, M., Röthlisberger, R., Ruth, U., Siggaard-Andersen, M.-L., Steffensen, J.P., Dahl-Jensen, D., Vinther, B.M., Clausen, H.B., 2006. The Greenland ice core chronology 2005, 15–42 ka. Part 1: constructing the time scale. *Quaternary Science Reviews* 25 (23–24), 3246–3257. <http://dx.doi.org/10.1016/j.quascirev.2006.08.002>.
- Bassinot, F., Labeyrie, L., 1995. IMAGES MD 101: A coring cruise of the R/V Marion Dufresne in the North Atlantic Ocean and Norwegian Sea. *l'Institut Français pour la Recherche et la Technologie Polaires, Plouzané, France*.
- Belcher, J., Hampton, J.S., Wilson, G.T., 1994. Parameterization of continuous time autoregressive models for irregularly sampled time series data. *Journal of the Royal Statistical Society, Series B (Methodology)* 56 (1), 141–155.
- Blunier, T., Brook, E.J., 2001. Timing of the millennial-scale climate change in Antarctica and Greenland during the Last Glacial Period. *Science* 291, 109–112. <http://dx.doi.org/10.1126/science.291.5501.109>.
- Bond, G.C., Lotti, R., 1995. Iceberg discharges into the North Atlantic on millennial time scales during the last glaciations. *Science* 267, 1005–1010.
- Bond, G.C., Broecker, W., Johnsen, S., McManus, J., Labeyrie, L., Jouzel, J., Bonani, G., 1993. Correlations between climate records from North Atlantic sediments and Greenland ice. *Nature* 365, 143–147.
- Bond, G.C., Showers, W., Elliot, M., Evans, M., Lotti, R., Hajdas, I., Bonani, G., Johnson, S., 1999. The North Atlantic's 1–2 kyr climate rhythm: relation to Heinrich events, Dansgaard/Oeschger cycles and the little ice age, mechanisms of global climate change at millennial time scales. *Geophysical Monograph* 112, 35–58.
- Braun, H., Ditlevsen, P., Kurths, J., Mudelsee, M., 2010. Limitations of red noise in analyzing Dansgaard–Oeschger events. *Climate of the Past* 6, 85–92.
- Braun, H., Ditlevsen, P., Kurths, J., Mudelsee, M., 2011. A two-parameter stochastic process for Dansgaard–Oeschger events. *Paleoceanography* 26, PA3214. <http://dx.doi.org/10.1029/2011PA002140>.
- Clement, A.C., Peterson, L., 2008. Mechanisms of abrupt climate change of the last glacial period. *Reviews of Geophysics* 46, RG4002. <http://dx.doi.org/10.1029/2006RG000204>.
- Dansgaard, W., Johnsen, S.J., Clausen, H.B., Dahl-Jensen, D., Gundestrup, N.S., Hammer, C.U., Hvidberg, C.S., Steffensen, J.P., Sveinbjörnsdóttir, A.E., Jouzel, J., Bond, G., 1993. Evidence for general instability of past climate from a 250-kyr ice-core record. *Nature* 364, 218–220.
- Dergachev, V.A., van Geel, B., 2004. Large-scale periodicity of climate change during the Holocene. In: Scott, E., et al. (Ed.), *Impact of the Environment of Human Migration in Eurasia*. Kluwer Academic Publishers, Dordrecht, Netherlands, pp. 159–183.
- Dima, M., Lohmann, G., 2009. Conceptual model for millennial climate variability: a possible combined solar-thermohaline circulation origin for the 1,500-year cycle. *Climate Dynamics* 32, 301–311. <http://dx.doi.org/10.1007/s00382-008-0471-x>.
- Ditlevsen, P.D., 1999. Observation of α -stable noise induced millennial climate changes from an ice-core record. *Geophysical Research Letters* 26, 1441–1444.
- Ditlevsen, P.D., Johnsen, S.J., 2010. Tipping points: early warming and wishful thinking. *Geophysical Research Letters* 37, L19703. <http://dx.doi.org/10.1029/2010GL044486>.
- Ditlevsen, P.D., Kristensen, M.S., Andersen, K.K., 2005. The recurrence time of Dansgaard–Oeschger events and limits on the possible periodic component. *Journal of Climate* 18, 2594–2603.
- Ditlevsen, P.D., Andersen, K.K., Svensson, A., 2007. The DO-climate events are probably noise induced: statistical investigation of the claimed 1470 years cycle. *Climate of the Past* 3, 129–134.
- Glynn, E.F., Chen, J., Mushegian, A.R., 2005. Detecting periodic patterns in unevenly spaced gene expression time series using Lomb–Scargle periodograms. *Bioinformatics* 22 (3), 310–316. <http://dx.doi.org/10.1093/bioinformatics/bti789>.
- Goldstein, S., Hemming, S., 2003. Long-lived isotopic tracers in oceanography, paleoceanography, and ice-sheet dynamics. In: Elderfield, H. (Ed.), *Treatise on Geochemistry*. The Oceans and Marine Geochemistry, 6. Elsevier, San Diego, California, pp. 453–489.
- Gorbarenko, S.A., Harada, N., Malakhov, M.I., Velivetskaya, T.A., Vasilenko, Y.P., Bosin, A.A., Derkachev, A.N., Goldberg, E.L., Ignatiev, A.V., 2012. Responses of the Okhotsk Sea environment and sedimentology to global climate changes at the orbital and millennial scale during the last 350 kyr. *Deep Sea Research Part II* 61–64, 73–84. <http://dx.doi.org/10.1016/j.dsr2.2011.05.016>.
- Grootes, P.M., Stuiver, M., 1997. Oxygen 18/16 variability in Greenland snow and ice with 10^{-3} to 10^3 -year time resolution. *Journal of Geophysical Research* 102 (C12), 26,455–26,470.
- Grootes, P.M., Stuiver, M., White, J.W.C., Johnsen, S., Jouzel, J., 1993. Comparison of oxygen isotope records from the GISP2 and GRIP Greenland ice cores. *Nature* 366, 552–554.
- Heinrich, H., 1988. Origin and consequences of cyclic ice rafting in the northeast Atlantic Ocean during the past 130,000 years. *Quaternary Research* 29, 142–145.
- Hemming, S.R., 2004. Heinrich events: massive late Pleistocene detritus layers of the North Atlantic and their global climate imprint. *Reviews of Geophysics* 42, RG1005. <http://dx.doi.org/10.1029/2003RG000128>.
- Hinnov, L.A., Schulz, M., Yiou, P., 2002. Interhemispheric space-time attributes of the Dansgaard–Oeschger oscillations between 100 and 0 ka. *Quaternary Science Reviews* 21, 1213–1228.
- Horne, J.H., Baliunas, S.L., 1986. A prescription for period analysis of unevenly sampled time series. *The Astrophysical Journal* 302, 757–763.
- Keigwin, L.D., Boyle, E.A., 1999. Surface and deep ocean variability in the northern Sargasso Sea during marine isotope stage 3. *Paleoceanography* 14 (2), 164–170.
- Koen, C., 2005. The analysis of irregularly observed stochastic astronomical time series – I. Basics of linear stochastic differential equations. *Monthly Notices of the Royal Astronomical Society* 361, 887–896. <http://dx.doi.org/10.1111/j.1365-2966.2005.09213.x>.
- Kwasniok, F., Lohmann, G., 2009. Deriving dynamical models from paleoclimate records: application to millennial-scale climate variability. *Physical Review E* 80, 066104.
- Liu, X.Y., Pei, L.Q., Zhang, S.M., Wang, Y., Dai, Y.D., 2011. Characteristics of magnetocardiography and electrocardiography in the time-frequency domain. *Chinese Science Bulletin* 56 (8), 819–825. <http://dx.doi.org/10.1007/s11434-010-4066-7>.
- Lomb, N.R., 1976. Least squares frequency analysis of unequally spaced data. *Astrophysics and Space Science* 39, 447–462.
- Meece, D.A., Alley, R.B., Fiacco, R.J., Germani, M.S., Gow, A.J., Grootes, P.M., Illing, M., Mayewski, P.A., Morrison, M.C., Ram, M., Taylor, K.C., Yang, Q., Zielinski, G.A., 1994. Preliminary depth-age scale of the GISP2 ice core. *Special CRREL Report 94-1*. US Army Corps of Engineers, Washington, D.C.
- Meece, D.A., Gow, A.J., Alley, R.B., Zielinski, G.A., Grootes, P.M., Ram, M., Taylor, K.C., Mayewski, P.A., Bolzan, J.F., 1997. The Greenland Ice Sheet Project 2 depth-age scale: methods and results. *Journal of Geophysical Research* 102 (C12), 26,411–26,423.
- Olsen, L., Hammer, Ø., 2005. A 6-ka climate cycle during at least the last 50,000 years. *Norges geologiske undersøkelse Bulletin* 445, 89–100.
- Pardo-Iguzquiza, E., Rodríguez-Tovar, F.J., 2011. Implemented Lomb–Scargle periodogram: a valuable tool for improving cyclostratigraphic research on unevenly sampled deep-sea stratigraphic sequences. *Geo-Marine Letters* 31, 537–545. <http://dx.doi.org/10.1007/s00367-011-0247-x>.
- Pisias, N.G., Clark, P.U., Brook, E.J., 2010. Modes of global climate variability during marine isotope stage 3 (60–26 ka). *Journal of Climate* 23, 1581–1588. <http://dx.doi.org/10.1175/2009JCLI3416.1>.
- Prahl, F.G., Wakeham, S.G., 1987. Calibration of unsaturation pattern in long-chain ketone compositions for paleotemperature assessment. *Nature* 330, 367–369.
- R Development Core Team, 2011. *R: A Language and Environment for Statistical Computing*. R Foundation for Statistical Computing, Vienna, Austria (Available: <http://www.R-project.org/>).
- Rahmstorf, S., 2002. Ocean circulation and climate during the past 120,000 years. *Nature* 419, 207–214.
- Rahmstorf, S., 2003. Timing of abrupt climate change: a precise clock. *Geophysical Research Letters* 30 (10), 1510. <http://dx.doi.org/10.1029/2003GL017115>.
- Rasmussen, S.O., Andersen, K.K., Svensson, A.M., Steffensen, J.P., Vinther, B.M., Clausen, H.B., Siggaard-Andersen, M.-L., Johnsen, S.J., Larsen, L.B., Dahl-Jensen, D., Bigler, M., Röthlisberger, R., Fischer, H., Goto-Azuma, K., Hansson, M.E., Ruth, U., 2006. A new Greenland ice core chronology for the last glacial termination. *Journal of Geophysical Research* 111, D06102. <http://dx.doi.org/10.1029/2005JD006079>.
- Ruf, T., 1999. The Lomb–Scargle periodogram in biological rhythm research: analysis of incomplete and unequally spaced time series. *Biological Rhythm Research* 30 (2), 178–201.
- Sachs, J.P., Lehman, S.J., 1999. Subtropical North Atlantic temperatures 60,000 to 30,000 years ago. *Science* 286, 756–759.

- Scargle, J.D., 1982. Studies in astronomical time series. II. Statistical aspects of spectral analysis of unevenly spaced data. *The Astrophysical Journal* 263, 835–853.
- Schulz, M., 2002. On the 1470-year pacing of the Dansgaard–Oeschger warm events. *Paleoceanography* 17 (2). <http://dx.doi.org/10.1029/2000PA000571>.
- Stuiver, M., Grootes, P.M., Braziunas, T.F., 1995. The GISP2 $\delta^{18}\text{O}$ climate record of the past 16,500 years and the role of the sun, ocean and volcanoes. *Quaternary Research* 44, 341–354. <http://dx.doi.org/10.1006/qres.1995.1079>.
- Svensson, A., Andersen, K.K., Bigler, M., Clausen, H.B., Dahl-Jensen, D., Davies, S.M., Johnsen, S.J., Muscheler, R., Rasmussen, S.O., Röthlisberger, R., Steffensen, J.P., Vinther, B.M., 2006. The Greenland ice core chronology 2005, 15–42 ka. Part 2: comparison to other records. *Quaternary Science Reviews* 25 (23–24), 3258–3267. <http://dx.doi.org/10.1016/j.quascirev.2006.08.003>.
- Svensson, A., Andersen, K.K., Bigler, M., Clausen, H.B., Dahl-Jensen, D., Davies, S.M., Johnsen, S.J., Muscheler, R., Parrenin, F., Rasmussen, S.O., Röthlisberger, R., Seierstad, I., Steffensen, J.P., Vinther, B.M., 2008. A 60 000 year Greenland stratigraphic ice core chronology. *Climate of the Past* 4, 47–57.
- Thomas, A.M., Rupper, S., Christensen, W.F., 2011. Characterizing the statistical properties and interhemispheric distribution of Dansgaard–Oeschger events. *Journal of Geophysical Research* 116, D03 103. <http://dx.doi.org/10.1029/2010JD014834>.
- Van Dongen, H.P.A., Olofsen, E., Van Harteveldt, J.H., Kruyt, E.W., 1999. A procedure of multiple period searching in unequally spaced time-series with the Lomb–Scargle method. *Biological Rhythm Research* 30 (2), 149–177.
- Vinther, B.M., Clausen, H.B., Johnsen, S.J., Rasmussen, S.O., Andersen, K.K., Buchardt, S.L., Dahl-Jensen, D., Seierstad, I.K., Siggard-Andersen, M.-L., Steffensen, J.P., Svensson, A., 2006. A synchronized dating of three Greenland ice cores throughout the Holocene. *Journal of Geophysical Research* 111, D13102. <http://dx.doi.org/10.1029/2005JD006921>.